Contrast Limits with the Simultaneous Differential Extrasolar Planet Imager (SDI) at the VLT and MMT

Beth A. Biller[a], Laird M. Close[a], Elena Masciadri[b], Rainer Lenzen[c], Wolfgang Brandner[c], Donald McCarthy[a], Thomas Henning[c], Eric L. Nielsen[a], Markus Hartung[d], Stephan Kellner[e], Kerstin Geissler[c], and Markus Kasper[f]

[a]Steward Observatory, University of Arizona, Tucson, AZ 85721, USA;
[b]Astrophysical Observatory of Arcetri - INAF, L. go E. Fermi 5, 50125 Firenze, Italy;
[c]Max-Planck-Institut für Astronomie, Königstuhl 17, 69117 Heidelberg, Germany;
[d]European Southern Observatory, Alonso de Cordova 3107, Santiago 19, Chile;
[e]W.M. Keck Observatory, 65-1120 Mamalohoa Highway, Kamuela, HI 96743, USA;
[f]European Southern Observatory, Karl-Schwarzschild-Strasse 2, D-85748 Garching, Germany

ABSTRACT

We discuss contrast limits obtained during a survey of young (<300 Myr), close (<50 pc) stars with the Simultaneous Differential Extrasolar Planet Imager (SDI) implemented at the VLT and the MMT. SDI uses a double Wollaston prism and a quad filter to take images simultaneously at 3 wavelengths surrounding the 1.62 μm methane bandhead found in the spectrum of cool brown dwarfs and gas giants. By performing a difference of images in these filters, speckle noise from the primary can be significantly attenuated, resulting in photon noise limited data. In our survey data, we achieved H band contrasts >25000 (5σ ΔF1(1.575μm)>10 mag, ΔH>10.6 mag for a T6 spectral type) at a separation of 0.5" from the primary star. With this degree of attenuation, we can image (5σ detection) a 2-4 Jupiter mass planet at 5 AU around a 30 Myr star at 10 pc. We are currently completing our survey of young, nearby stars. We have obtained complete datasets for 40 stars in the southern sky (VLT) and 11 stars in the northern sky (MMT). We believe that our SDI images are the highest contrast astronomical images ever made from ground or space for methane rich companions.

Keywords: high contrast imaging, adaptive optics, extrasolar planets, simultaneous differential imaging

1. INTRODUCTION

Direct detection of extrasolar giant planets is extremely difficult. Giant gas planets seen in reflected light are >20 magnitudes fainter than their primary stars and likely lie within ~1" of their primary stars. The problem is slightly easier with younger, hotter planets – 100 Myr old extra-solar planets are 10^{4-7} times more self-luminous than old (5 Gyr) extra-solar planets, whereas their primary stars are only slightly (2-5 times) brighter at early ages. In theory, adaptive optics (AO) systems that are "photon noise limited" can detect an object up to 10^5 times fainter than its primary at separations >1". However, numerous surveys for extrasolar planets using large telescopes with AO systems have yielded useful limits but few confirmed giant planet candidates (Kaisler et al. 2003, Masciadri et al. 2005, Chauvin et al. 2005, Neuhäuser et al. 2005).

AO surveys for young extrasolar planets only address half of the difficulty of direct detection – the contrast limit problem. Beyond the contrast limit problem, all AO systems suffer from a limiting "speckle noise" floor (Racine et al. 1999). Within 1" of the primary star, the field is filled with speckles left over from instrumental features and residual atmospheric turbulence after adaptive optics correction. These speckles vary as a function of time and color. For photon noise limited data, the signal to noise S/N is proportional to $t^{0.5}$, where t is the exposure time. For speckle-noise limited data, the S/N does not increase with time past a specific speckle-noise floor (limiting contrasts to ~10^3 at 0.5"). This speckle-noise floor is considerably above the photon noise limit and makes planet detection very difficult. Interestingly, space telescopes such as HST also suffer from

Further author information: (Send correspondence to B.A.B.)
B.A.B.: E-mail: bbiller@as.arizona.edu, Telephone: 1 520 621 2589

Advances in Adaptive Optics II, edited by Brent L. Ellerbroek, Domenico Bonaccini Calia,
Proc. of SPIE Vol. 6272, 62722D, (2006) · 0277-786X/06/$15 · doi: 10.1117/12.671771

a similar limiting speckle-noise floor due to imperfect optics and "breathing" (Schneider et al. 2003). Direct detection of extrasolar giant planets requires special new instrumentation to suppress this speckle noise floor and produce photon noise limited images. The VLT, Subaru, and Gemini are all currently developing dedicated planet-finding cameras which exploit these new instrumentational approaches for speckle suppression. The Simultaneous Differential Imager (SDI), which our team built and installed at the VLT and MMT, is one of the first dedicated planet-finding instruments to come online (Close et al. 2005, Lenzen et al. 2004, Lenzen et al. 2005).

Simultaneous Differential Imaging is an instrumental method which can be used to calibrate and remove the "speckle noise" in AO images, while also isolating the planetary light from the starlight. This method was pioneered by Racine et al. (1999), Marois et al. (2000), Marois et al. (2002), and Marois et al. (2005). It exploits the fact that all cool (T_{eff} <1200 K) extra-solar giant planets have strong CH_4 (methane) absorption redwards of 1.62 μm in the H band infrared atmospheric window (Burrows et al. 2001, Burrows et al. 2003). Our SDI device obtains four images of a star simultaneously through three slightly different narrowband filters (sampling both inside and outside of the CH_4 features). These images are then differenced. This subtracts out the halo and speckles from the bright star to reveal any massive extrasolar planets orbiting that star. Since a massive planetary companion will be brightest in one filter and absorbed in the rest, while the star is bright in all three, a difference can be chosen which subtracts out the star's light and reveals the light from the companion. Thus, SDI also helps eliminate the large contrast difference between the star and substellar companions (Close et al. 2005; Lenzen et al. 2004; Lenzen et al. 2005) The SDI device has already produced a number of important scientific results: the discovery of AB Dor C (Close et al. 2005) which is the tightest (0.16") low mass companion known, the discovery of SCR 1845-6357B, a very nearby (3.85 pc) T5.5 brown dwarf orbiting an M8.5 star (Biller et al. 2006a), evidence of orbital motion for Gl 86B, the first known white dwarf companion to an exoplanet host star (Mugrauer and Neuhäuser 2005), the first high-contrast surface maps of Titan (Hartung et al. 2004), and the discovery of ϵ Indi Ba-Bb, the nearest binary brown dwarf (McCaughrean et al. 2005).

2. THE SDI AO CAMERAS AT THE VLT AND MMT

An SDI imaging scheme is currently implemented at the 6.5m MMT (using the MMT AO adaptive secondary mirror and the ARIES AO camera – McCarthy et al. 1998) and at the ESO VLT (using the 8m UT4 and the NAOS-CONICA (NACO) AO system) by a group headed by L. Close and R. Lenzen (Close et al. 2005, Lenzen et al. 2004, Lenzen et al. 2005).

The SDI technique requires some specialized optics consisting of a cryogenic custom double calcite Wollaston device and a focal plane quad CH_4 filter. Our custom Wollaston splits the beam into four identical beams while minimizing non-common path errors. The *differential* non-common path errors are less than 20 nm RMS per Zernike mode (Lenzen et al. 2004). Each of the four beams is fed through one of the filters on the quad filter. Filter wavelengths were chosen on and off the methane absorption feature at 1.62 μm and were spaced closely (every 0.025 μm) in order to limit residuals due to speckle and calcite chromatism. We used four filters F1, F2, F3a, and F3b with central wavelengths F1=1.575 μm, F2=1.600 μm, and F3a=F3b=1.625 μm. The filters have bandwidths of 0.025 μm. A cold 5"×5" focal plane mask has been implemented as a field stop for the VLT device. No coronagraph is currently used, since the Strehl ratios (~20-30%) are too low to increase the contrasts significantly. The SDI camera has a platescale of 0.017″/pix.

3. OBSERVATIONAL TECHNIQUE AND DATA REDUCTION

A 2 minute long on-sky raw dataset from NACO SDI is shown in Fig. 1. The inner 0.2" diameter core is saturated in each image to increase signal in the halo. After unsharp masking, we find that the speckle patterns in each of the separate filters are nearly identical (see Fig. 1), which makes effective speckle attenuation possible through differential imaging. Two minute long raw datasets were taken for each object observed at 4-5 different dither positions. In order to distinguish between faint planets and any residual speckles, we repeated the observations for each object at a variety of position angles. Instrumental and telescope "super speckles" (Racine et al. 1999) should not rotate with a change of rotator angle; however, a real planet should appear to rotate by the change in rotator angle.

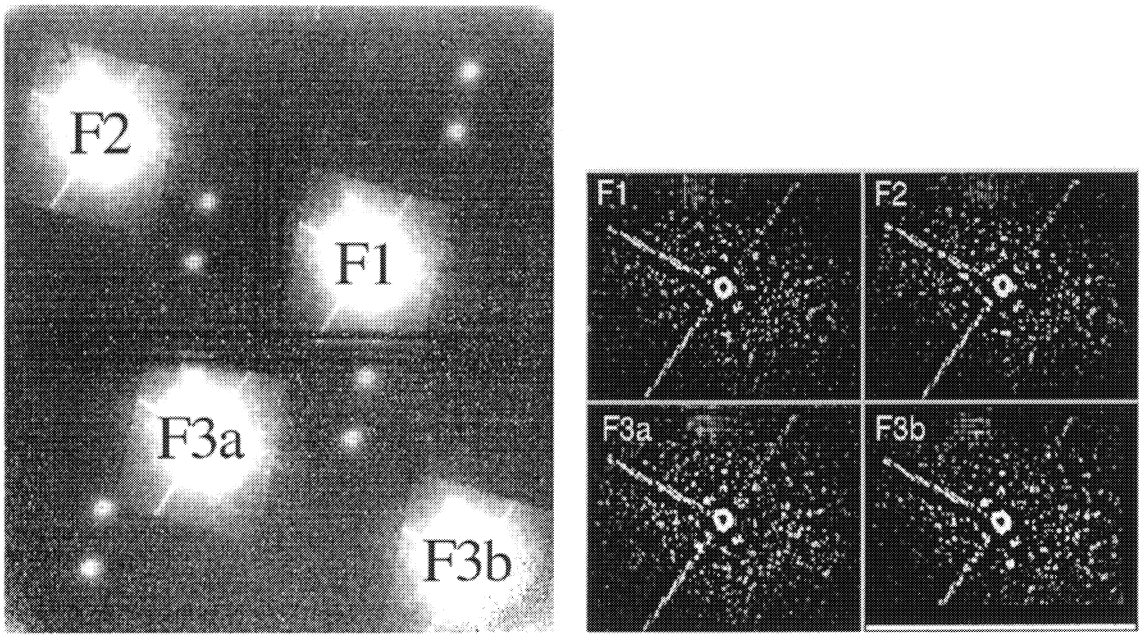

Figure 1. Left: Two minutes of raw SDI data on the 1024×1024 Aladdin array in the NACO AO camera (Rousset et al. 2003, Lenzen et al. 2003, Lenzen et al. 2004). Note that the field mask is tilted and that electronic ghosts are visible due to overexposure. Each saturated spot produces three ghosts (axis- and point-) symmetrical to the center of the detector. The source is saturated on purpose to enhance the signal to noise of a potential companion. The source appears comparably bright in all four filters. Right: Same dataset, slightly processed. Apertures have been selected around each filter image. In order to reveal the speckle pattern, a heavily smoothed image was subtracted from the raw images (unsharp masking). The resulting speckle patterns are very similar between the 4 simultaneous images which means that an effective subtraction of speckles can be obtained between the filters.

Each raw data frame is reduced using a custom IDL script. A pipeline block diagram for this IDL script is presented in Figs. 2. After basic data processing (sky subtraction, flat field correction, and bad pixel removal), an aperture is extracted around each filter image. In each aperture, the Airy pattern and total image flux is scaled to that of a reference image. Images in different filters are then aligned using a custom shift and subtract algorithm. We calculate 2 differences (and one non-differenced combination) which are sensitive to substellar companions of spectral types "T" ($T_{eff} < 1200$ K), "Y" ($T_{eff} \leq 600$ K), and "L" ($T_{eff} > 1200$ K). Data taken at different position angles are subtracted (e.g. 20 minutes of data at 0 degrees minus 20 minutes of data at 33 degrees) in order to further attenuate speckle noise.

To illustrate the signal produced by an object with a strong methane absorption break, images of SCR 1845-6357A and B are presented in Fig. 3. SCR 1845-6357B is a very nearby M8.5 star (3.85 pc). We recently discovered a T5.5 brown dwarf companion to the M8.5 star using the SDI device (Biller et al. 2006a). In this discovery image, the M8.5 primary appears strong in all four filters, while the flux of T5.5 companion drops by a factor of 3 in the 1.625 μm methane absorption filters. In the full SDI data reduction (reduction algorithm described below) of the entire dataset (right panel of Fig. 3), the T5.5 companion appears with a characteristic dark/light pattern (dark and light images separated by the roll angle between observation) and the speckles from the M8.5 primary are almost totally removed. With the high contrasts achievable by SDI, a methane object like SCR 1845B (ΔH=4.2 mag) could have been detected at 10σ 10× closer in at a separation of only ~0.1".

A fully reduced dataset from the VLT SDI device as well as the same dataset reduced in a standard AO manner is presented in Fig. 4. This is 40 minutes of data for AB Dor A, a 70 Myr K1V star at a distance of 14.98 pc (V=6.88). Simulated planets were inserted into the dataset pre-reduction at separations of 0.55, 0.85, and 1.35" from the primary, with ΔF1 = 10 mag (attenuation in magnitudes in the F1 1.575 μm filter) fainter

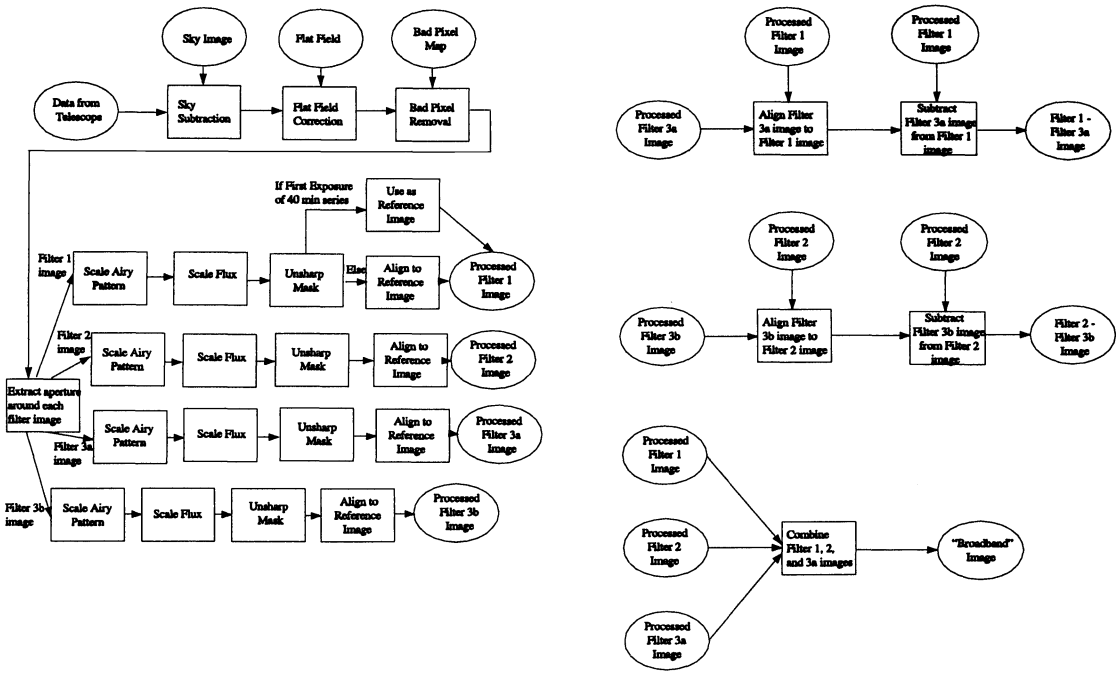

Figure 2. Pipeline Block Diagrams

than the primary. These planets are scaled from unsaturated images of the example star taken right before the example dataset (and have fluxes and photon noise in each filter appropriate for a T6 object). In the SDI reduction, the simulated planets are detected with S/N > 10 past 0.7". In comparison, none of the simulated planets are detected in the standard AO data reduction and numerous bright super speckles remain in the field.

A plot of ΔF1 (5σ) vs. separation from the primary is presented in Fig. 5. For this dataset, we achieved star to planet H band contrasts (5σ) >25000 (5σ ΔF1(1.575 μm) > 10.0 mag, ΔH>10.6 mag for a T6 spectral type object) at a separation of 0.5" from the primary star – approaching the photon-noise limit in 40 minutes of data.

4. CONTRAST LIMITS AND PLANET DETECTABILITY FROM THE SDI SURVEY

We are currently completing a survey with the SDI device of ~50 young (<300 Myr), nearby (<50 pc) stars (Biller et al. 2006c). Stars were chosen based on strong lithium absorption features (our best targets have Li equivalent widths of >100 mÅ from the Li 6707 Å line, generally corresponding to age < 100 Myr) and accurate Hipparcos parallax measurements (parallaxes of > 0.02", corresponding to distances < 50 pc). Complete datasets have been acquired for 50 stars total – 40 stars in the southern sky and 11 stars in the northern sky (some stars were observed in both the north and the south). The "average" survey object is a late K star with an age of 120 Myr and at a distance of 26 pc.

To estimate the range of star-planet contrasts achievable in our SDI young stars survey, we consider three example cases which span the space of our target stars: case A – a high quality dataset (observed with seeing of ~0.5"), case B – AB Dor A, a bright young solar analogue, and case C, a faint young M star. Properties of each example star (distance, age, spectral type, etc.) are presented in Table 1. Contrast curves were generated from the subtracted image by tracking a 6×6 pixel box along a straight line leading radially away from the source in a specified direction (usually chosen to avoid spider arm residuals). For each position along the selected trajectory, we calculate the standard deviation in that box. ΔF1 (5σ attenuation in magnitudes in the 1.575 μm F1 filter) vs.

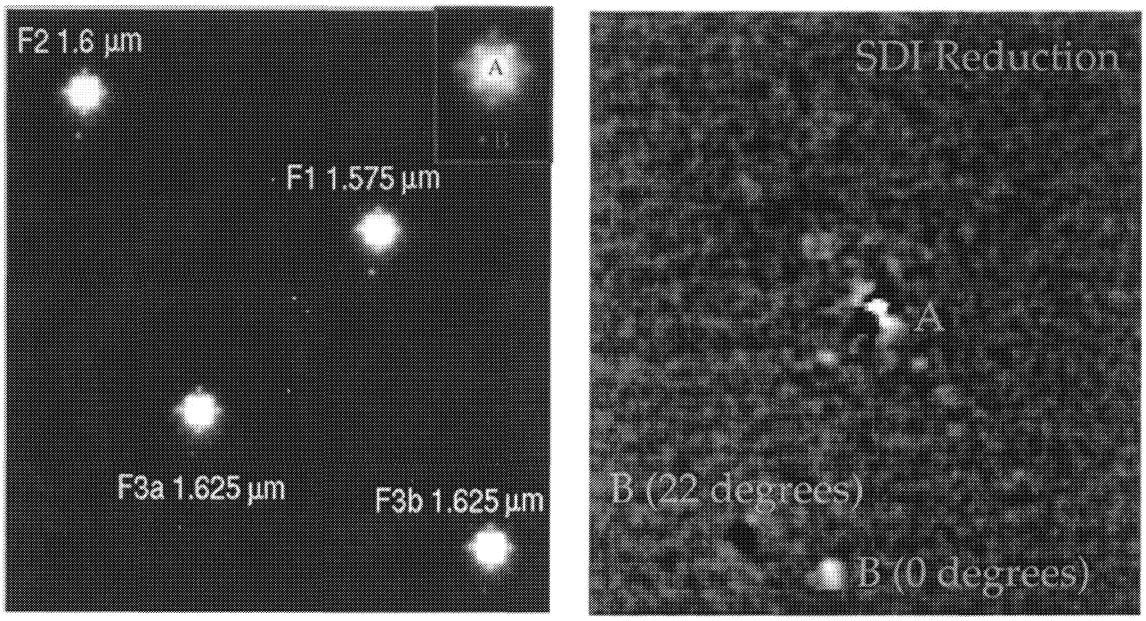

Figure 3. SDI images of SCR 1845. **Left:** 15 minute long image taken at a position angle of 0°. A substellar companion appears at a separation of 1.170"±0.003" (4.5 AU at 3.85 pc) from the primary and a position angle of 170.20±0.13° in each of the 4 SDI filters. The platescale is (0.01725"±0.00025") / pix (Nielsen et al. 2006). The companion appears brightest in the F1 filter (out of the CH_4 absorption) and drops by a factor of 2.7 in the F3 filter (inside the CH_4 absorption), consistent with a T5.5 dwarf spectral type. North is up and east is to the left. **Inset:** Three color image of SCR 1845 A and B generated from the SDI filter images (blue=1.575 μm, green=1.600 μm, red=1.625 μm). The substellar companion appears blue in this image. This image was created with a log10 stretch and each filter is equally weighted. Note how similar in color (white) each of the PSF speckles are for the M8.5, while the faint companion SCR 1845B is considerably bluer due to strong CH_4 absorption. The structure in the PSF is typical of the NACO IR WFS for a faint guide star such as SCR 1845A. **Right:** Images of SCR 1845 using the SDI device and reduced using a custom SDI pipeline (Biller et al. 2006b). This 30 minute long image was taken at position angles of 0° (white) and 22° (black). Datasets from each roll angle were subtracted from each other and smoothed with a 1 pixel FWHM gaussian. A substellar companion appears at a separation of 1.17" from the primary in each of the 4 SDI filters. Note that the speckles from the M8.5 are almost totally removed. With the high contrasts achievable by SDI, a methane object like SCR 1845B (ΔH=4.2 mag) could have been detected at 10σ 10× closer in at a separation of only ~0.1".

Table 1. Properties of Example SDI Survey Stars and Comparison Stars

Case	Spectral Type	Age	Distance	H	V	Exposure Time	ΔF1[1]	ΔH[1]
A	K2V	30 Myr	45.5 pc	7.1	9.1	40 min	10.5	11.1
B	K1V	70 Myr	15 pc	4.8	6.9	40 min	10.5	11.1
C	M3V	30 Myr	24 pc	7.1	12.2	40 min	10	10.6
15 late K-M stars[2]	K-M	<50 Myr	10-50 pc	6.4-8.7	8-12	20 min	8.61	10.31[4]
Gl 86[3]	K1V	10 Gyr	10.9 pc	4.2	6.2	80 min	12.8	13.4

[1] 5σ at 0.5" [2] Masciadri et al. 2006 [3] Mugrauer & Neuhäuser 2005
[4] Updated value: ΔH = 9.21 (using Offset$_{T6}$ = 0.6±0.07 mag, see text)

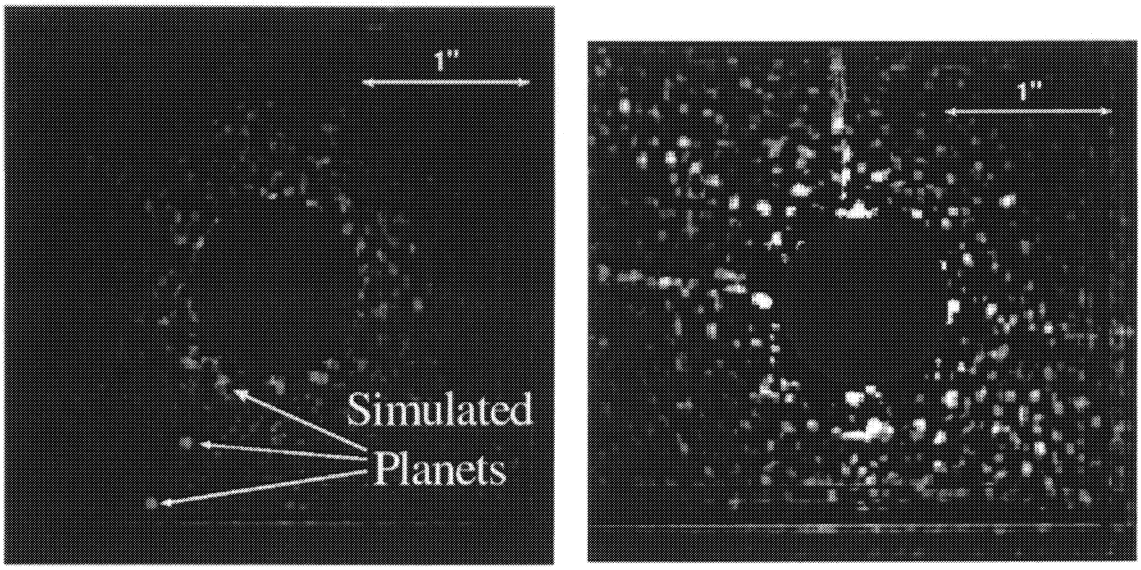

Figure 4. Left: A complete reduced dataset (40 minutes of data at a series of rotator angles – 0°, 33°, 33°, 0°) from the VLT SDI device. Simulated planets have been added at separations of 0.55, 0.85, and 1.35" from the primary, with ΔF1(1.575μm) = 10 mag (attenuation in magnitudes in the 1.575 μm F1 filter) fainter than the primary. These planets are scaled from unsaturated images of the example star taken right before the example dataset (and have fluxes and photon noise in each filter appropriate for a T6 object). Past 0.7", the simulated planets are detected with S/N > 10. Right: Standard AO data reduction of the same dataset. Filter images have been coadded (rather than subtracted), flat-fielded, sky-subtracted, and unsharp-masked. Simulated planets have been added with the same properties and at the same separations as before. None of the simulated planets are detected in the standard AO reduction. Additionally, numerous bright super speckles remain in the field.

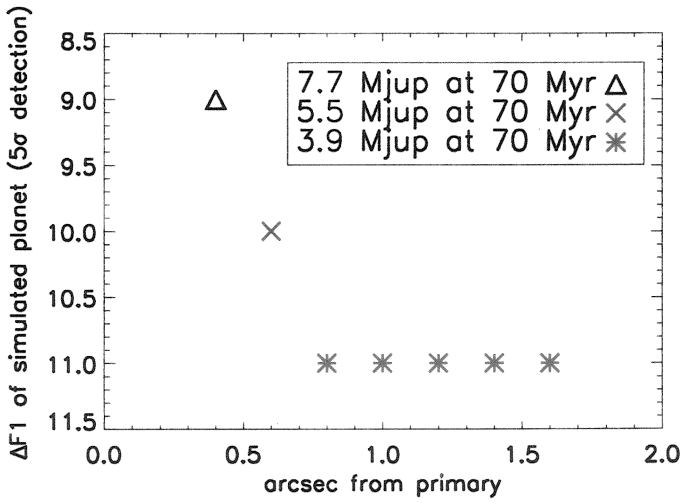

Figure 5. Minimum Detectable Planet Mass (5σ detection vs. Separation for 40 minutes of VLT SDI data for Case B). Tob determine minimum detectable planet mass as a function of separation, we inserted and then attempted to retrieve simulated planets with a variety of separations and ΔF1 contrasts. ΔF1 contrasts were translated into planet masses using the models of Burrows et al. 2003. For this particular star, we can detect a 5 M_{Jup} planet 12 AU from the star.

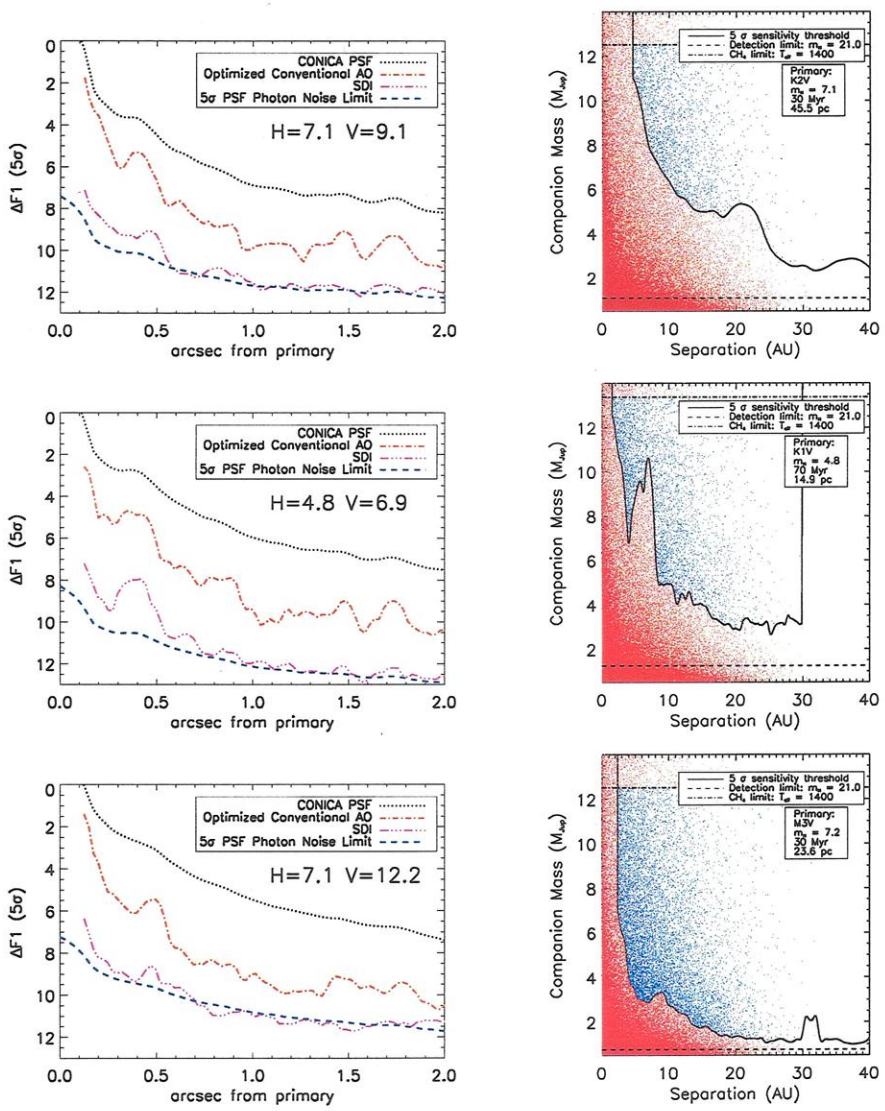

Figure 6. Top: Case A, Middle: Case B, Bottom: Case C. Left: ΔF1 (5σ attenuation in magnitudes in the 1.575 μm F1 filter) vs. Separation for 40 minutes of VLT SDI data for each example star. The top curve is the AO PSF. The next curve is the "classical AO PSF" unsharp masked. The third curve down is 40 minutes of SDI data taken at two different position angles and subtracted (0° data -33° data). The last curve is the theoretical contrast limit due to photon-noise. For each case, at star-companion separations >0.5", we are photon-noise limited and achieve H band star to planet contrasts >25000 (5σ ΔF1(1.575μm)>10 mag, ΔH>10.6 mag for a T6 spectral type) Right: Minimum Detectable Planet Mass vs. Separation – using the models of Burrows et al. (2003) and primary star properties from the literature, we can convert our ΔF1 values into a minimum detectable planet mass for each object. Objects above the 1400 K methane cutoff line (horizontal dashed line) are not detected with the SDI device. For details, see Nielsen et al. 2006.

separation from the primary is presented for each of the example cases in Fig. 6. To convert between our F1 filter fluxes and H band magnitudes, we must take into account the spectrum of the companion object. A methane-rich object will be strong in some parts of the H band (filters F1 and F2) and weak in others, due to absorption (in filter F3 and redwards). This spectral dependence will correspond to a magnitude offset between our F1 band and the standard H band. In this case, a methane object will appear brighter in the F1 filter than in the full H band. Previously, we estimated a magnitude offset $\text{Offset}_{T6} = 1.7$ for a T6 companion from the methane band break strength of the T6 brown dwarf Gl 299B (Biller et al. 2006c). This offset corresponds to the constant A = 1.7 used to comple Table 1 in Masciadri et al. 2006. However, Gl 229B actually possesses anomalously high methane absorption compared to other objects of its spectral type (Geballe et al. 2002). An updated magnitude offset was calculated using spectra of 15 objects with spectral types of T4.5-T7 an H band transmission curve, and our F1 filter transmission curve (see Biller et al. 2006a). Using this method, we calculated magnitude offsets of $\text{Offset}_{T5} = 0.5 \pm 0.05$ for a T5 companion and $\text{Offset}_{T6} = 0.6 \pm 0.07$ for a T6 companion. The primary star is assumed to be nearly constant in flux across the H band. For our example datasets, we achieved H band star to planet contrasts >25000 (5σ ΔF1(1.575μm)>10 mag, ΔH>10.6 mag for a T6 spectral type) at a separation of 0.5" from the primary star – approaching the photon-noise limit in 40 minutes of data.

Using the models of Burrows et al. (2003) and adopting values for the primary star's age (from the Li 6707 Å line or moving group membership), distance, and spectral type from the literature, we can convert our measured attenuations for each object into a minimum detectable mass (see Nielsen et al. 2006). Minimum detectable mass vs. separation for each of the examples is also presented in Fig. 6. Although we achieve similar contrast limits for our example cases (with slightly higher contrasts for brighter targets as one might expect), the mass and separation of objects detectable around each varies strongly with age and distance. Even though case A was our best quality data, we are more likely to detect planets for case B and C, simply because these two objects are closer to the sun, and hence, we can resolve the inner ~20 AU around the star. For case C, we can detect (>5σ) a 3-5 M_J planet at 6 AU from the primary. ΔF1 and ΔH (for a methane object) for each survey case as well as for other comparison objects from the literature are shown in Table 1 – it is clear that the achievable contrast varies according to the magnitude of the object and total exposure time.

To determine what sort of objects we can realistically detect with this level of contrast, we inserted and then attempted to retrieve simulated T6 dwarf planets to the case B dataset with a variety of separations and ΔF1 contrasts. ΔF1 contrasts were translated into planet masses using the models of Burrows et al. 2003. In Fig. 5, we plot minimum detectable planet mass (for a 5σ detection) vs. separation. For this particular star (case B: K1V, 70 Myr, 15 pc), we can detect a 5 M_{Jup} planet 12 AU from the star. In this particular case we were able to detect a non-methane companion (AB Dor C) at 3 different epochs and separations from 0.15" to 0.2" even though ΔH>5 mag (Close et al. 2005b, Nielsen et al. 2006).

5. CONCLUSIONS

The novel SDI device at the VLT and MMT has been fully commissioned and is currently achieving attenuations of >25000 (ΔH > 10.6 for a T6 spectral type object, ΔF1(1.575μm)>10 at 0.5"). With these contrasts, we can detect a wide range of substellar objects. For instance, for AB Dor A (a 70 Myr K1V star 15 pc away) we can detect (>5 σ) a 5 M_{Jup} planet 12 AU from the star. For a younger closer star (30 Myr age at 10 pc), we can detect a 2-4 M_{Jup} planet at 5 AU.

We have currently observed ~50 of the youngest (<300 Myr), nearest (<50 pc) stars as part of a survey of young, nearby stars. We have received data from the VLT for followup of 8 tentative candidates found as part of the survey. None of the candidates were confirmed in this data set. With a total sample size of ~50 stars, we will be able to place strong constraints on the frequency and semimajor axis distribution of massive extrasolar planets >5 AU from their primaries. From scaling laws derived from the distribution of known radial velocity planets (Marcy et al. 2003, Lineweaver and Grether 2003, Burrows et al. 2003), we expect to detect ~4 planets for our total sample (see Nielsen et al. 2006). Whether or not we detect planets, our survey will begin to measure the true distribution young massive extrasolar planets >5 AU from their primaries and will provide valuable contraints for theories of planet formation and migration.

ACKNOWLEDGMENTS

BAB acknowledges support through the NASA GSRP program. LMC acknowledges support through NSF CAREER and NASA Origins grants. ELN is supported by the Michelson Fellowship.

REFERENCES

1. B.A. Biller, M. Kasper, L.M. Close, W. Brandner, and S. Kellner, "Discovery of a Brown Dwarf Very Close to the Sun: A Methane-Rich Brown Dwarf Companion to the Low-Mass Star SCR 1845-6357," *Astrophysical Journal* **641**, pp. L141 – L144, 2006a
2. B.A. Biller, L.M. Close, R. Lenzen, W. Brandner, D. McCarthy, E. Nielsen, S. Kellner, and M. Hartung, "Suppressing Speckle Noise for Simultaneous Differential Extrasolar Planet Imaging (SDI) at the VLT and MMT," in *Direct Imaging of Exoplanets: Science and Techniques. Proceedings of the IAU Colloquium #200*, pp. 571 – 576, 2006b
3. B.A. Biller, L.M. Close, E. Masciadri, R. Lenzen, W. Brandner, D. McCarthy, T. Henning, E. Nielsen, and M. Hartung, "A Survey of Close, Young Stars with SDI at the VLT and MMT," in *Direct Imaging of Exoplanets: Science and Techniques. Proceedings of the IAU Colloquium #200*, pp. 53 – 60,2006c
4. A. Burrows, W. B. Hubbard, J. Lunine, and J. Liebert, "The Theory of Brown Dwarfs and Extrasolar Giant Planets ," *Reviews of Modern Physics* **73**, pp. 719 – 765 , 2001
5. A. Burrows, D. Sudarsky, and J. Lunine, "Beyond the T Dwarfs: Theoretical Spectra, Colors, and Detectability of the Coolest Brown Dwarfs," *Astrophysical Journal* **596**, pp. 587 – 596 , 2003
6. G. Chauvin, A.-M. Lagrange, C. Dumas, B. Zuckerman, D. Mouillet, I. Song, J.-L. Beuzit and P. Lowrance, "Giant Planet Companion to 2MASSW J1207334-393254," *Astronomy and Astrophysics* **438**, pp. L25 – L28, 2005
7. L. Close, R. Lenzen, B. Biller, W. Brandner, and M. Hartung, "Selected Examples of Solar and Extra-solar Planetary Science with AO," in *Science with AO ESO Workshop September 16-19 2003*, pp. 136, 2005a
8. L.M. Close, R. Lenzen, J.C. Guirado, E.L. Nielsen, E.E. Mamajek, W. Brandner, M. Hartung, C. Lidman, and B. Biller, "A Dynamical Calibration of the Mass-Luminosity Relation at Very Low Stellar Masses and Young Ages," *Nature* **433**, pp. 286 – 289, 2005b
9. T. Geballe et al., "Toward Spectral Classification of L and T Dwarfs: Infrared and Optical Spectroscopy and Analysis," *Astrophysical Journal* **564**, pp. 466 – 481, 2002
10. M. Hartung, T.M. Herbst, L.M. Close, R. Lenzen, W. Brandner, O. Marco, and C. Lidman, "A New VLT Surface Map of Titan at 1.575 microns," *Astronomy and Astrophysics* **421**, pp. L17 – L20, 2004
11. D. Kaisler, B. Zuckerman, and E. Becklin, "A Keck Adaptive Optics Search for Young Extrasolar Planets," in *Scientific Frontiers in Research on Extrasolar Planets, ASP Conference Series* **294**, pp. 91 – 94, 200
12. R. Lenzen, M. Hartung, W. Brandner, G. Finger, N.N. Hubin, F. Lacombe, A.-M. Lagrange, M.D. Lehnert, A.F.M. Moorwood, and D. Mouillet, "NAOS-CONICA First On Sky Results in a Variety of Observing Modes," *Proc.SPIE* **4841**, pp. 944 – 952, 2003
13. R. Lenzen, L. Close, W. Brandner, M. Hartung, and B. Biller, "A Novel Simultaneous Differential Imager for the Direct Imaging of Giant Planets," *Proc. SPIE* **5492**, pp. 970 – 977, 2004
14. R. Lenzen, L. Close, W. Brandner, M. Hartung, and B. Biller, "NACO-SDI: A Novel Simultaneous Differential Imager for the Direct Imaging of Giant Extra-Solar Planets," in *Science with AO ESO Workshop September 16-19 2003*, pp. 46, 2005
15. C.H. Lineweaver and D. Grether, "What Fraction of Sun-like Stars have Planets?" *Astrophysical Journal* **598**, pp. 1350 – 1360, 2003
16. G. Marcy, R. Butler, D. Fischer, and S. Vogt, "Properties of Extrasolar Planets," in *Scientific Frontiers in Research on Extrasolar Planets, ASP Conference Series* **294**, pp. 1 – 16, 2003
17. C. Marois, R. Doyon, R. Racine, and D. Nadeau, "Efficient Speckle Noise Attenuation in Faint Companion Imaging," *Proceedings of the Astronomical Society of the Pacific* **112**, pp. 91 – 96, 2000
18. C. Marois, R. Doyon, R. Racine, and D. Nadeau, "Differential Imaging Coronagraph for the Detection of Faint Companions," *Proc. SPIE* **4008**, pp. 788 – 796, 2002

19. C. Marois, R. Doyon, D. Nadeau, R. Racine, M. Riopel, P. Vallée, and D. Lafrenière, "TRIDENT: An Infrared Differential Imaging Camera Optimized for the Detection of Methanated Substellar Companions," *Proceedings of the Astronomical Society of the Pacific* **117**, pp. 745 – 756, 2005
20. E. Masciadri, R. Mundt, T. Henning, C. Alvarez, and D. Barrado y Navascués, "A Search for Hot Massive Extrasolar Planets around Nearby Young Stars with the Adaptive Optics System NACO," *Astrophysical Journal* **625**, pp. 1004 – 1018, 2005
21. E. Masciadri, K. Geissler, S. Kellner, W. Brandner, T. Henning, R. Mundt, L. Close, B.A. Biller, and A. Raga, "Ground-Based Direct Imaging of Extra-Solar Planets Supported by AO," in *Direct Imaging of Exoplanets: Science and Techniques. Proceedings of the IAU Colloquium #200*, pp. 501 – 506, 2006
22. M.J. McCaughrean, L.M. Close, R.-D. Scholz, R. Lenzen, B. Biller, W. Brandner, M. Hartung, and N. Lodieu, "Epsilon Indi Ba, Bb: The Nearest Binary Brown Dwarf," *Astronomy and Astrophysics* **413**, pp. 1029 – 1036, 2003
23. D. McCarthy, J. Burge, R. Angel, J. Ge, R. Sarlot, B. Fitz-Patrick, and J. Hinz, "ARIES: Arizona Infrared Imager and Echelle Spectrograph," *Proc. SPIE* **3354**, pp. 750 – 754, 1998
24. M. Mugrauer and R. Neuhäuser, "GL86B: A White Dwarf Orbits an Exoplanet Host Star," *Monthly Notices of the Royal Astronomical Society* **361**, pp. L15 – L19, 2005
25. R. Neuhäuser, E.W. Guenther, G. Wuchterl, M. Mugrauer, A. Bedalov, and P.H. Hauschildt, "Evidence for a co-moving sub-stellar companion of GQ Lup," *Astronomy and Astrophysics* **435**, pp. L13 – L16, 2005
26. E. Nielsen, L.M. Close, and B.A. Biller, "Simulating Extrasolar Planet Populations for Direct Imaging Surveys," in *Direct Imaging of Exoplanets: Science and Techniques. Proceedings of the IAU Colloquium #200*, pp. 111 – 118, 2006.
27. R. Racine, G.A.H. Walker, D. Nadeau, R. Doyon, and C. Marois, "Speckle Noise and the Detection of Faint Companions," *Proceedings of the Astronomical Society of the Pacific* **111**, pp. 587 – 594, 1999
28. G. Rousset, F. Lacombe, P. Puget, N.N. Hubin, E. Gendron, T. Fusco, R. Arsenault, J. Charton, P. Feautrier, P. Gigan, P.Y. Kern, A.-M. Lagrange, P.-Y. Madec, D. Mouillet, D. Rabaud, P. Rabou, E. Stadler, and G. Zins, "NAOS, the first AO system of the VLT: on-sky performance," *Proc. SPIE* **4839**, pp. 140 – 149, 2003
29. G. Schneider, E. Becklin, L. Close, D. Figer, J. Lloyd, B. Macintosh, D. Hines, C. Max, D. Potter, M. Rieke, N. Scoville, R. Thompson, A. Weinberger, and R. Windhorst. "Domains of Observability in the Near-Infrared with HST/NICMOS and (Adaptive Optics Augmented) Large Ground-Based Telescopes," *solicited by STScI in preparation for HST Cycle 12*, 2003